Modeling of Diffusive and Premixed Flame of AP/HTPB Laminate Propellant

F. Maggi, L. T. DeLuca, G. Colombo, A. Bandera, and L. Galfetti
SPLab, Dipartimento di Energetica, Politecnico di Milano, 20156 Milan, Italy

Abstract

Composite propellants feature a diffusive flame. The size of oxidizer particles leverage some combustion properties (mainly burning rate and pressure sensitivity) along with flame structure. Macroscopic combustion features are strictly related to those events occurring inside the gas phase and close to the burning surface. The flame of nonaluminized composite energetic materials is considered and a simplified combustion model is tested on that. We simulate the combustion of a laminate propellant with varying lamina size. The benchmark consists of some movies taken from AP/HTPB propellant combustion with a high speed video camera. Three different powder sizes are used in propellant manufacturing.

1. Introduction

The flame of a composite propellant is a complex dynamic system that encompass heat transfer, chemistry, chemical diffusion, etc. Its nature is strictly joint to the features of condensed phase. An AP-based propellant is a multiphase system. This material has an intrinsic heterogeneous nature from a microscopic point of view. The simplest composition contains AP (ammonium perchlorate) powder and a polymeric binder like HTPB (hydroxy-terminated polybutadiene). AP decomposes into oxidizing gases while binder pyrolysis produces fuel gases. In addition, a propellant can contain some metal powder as a fuel (like aluminum) and other minor additives like iron oxide, ammonium bichromate, etc. Nonaluminized propellants have by far a simpler flame structure than those metalized because they are free from particle agglomeration issues. This was the reason for they were mainly addressed since initial studies on flame structure and they are still too. This simple configuration is featured by a complicated flame structure. Ammonium perchlorate decomposes into a reactive mixture which can be partly consumed by a premixed flame if pressure is over 20 bar.[1] This reaction is mainly driven by kinetic issues and combustion products are still reactive and hot.[2] Pure AP cannot sustain a deflagration wave when pressure is set under 20 bar but inside a propellant AP decomposition products interact also along with light-weight hydrocarbon gases from binder pyrolysis.[3] The resulting mixture is highly flammable also under sub-atmospheric conditions. This flame is diffusive. Moreover random displacement of AP inside the polymer matrix yields to unsteady flame structure. In fact, during combustion surface composition keeps on changing locally and the flame is effectively non-stationary, but only from a microscopic point of view. Plenty of models were developed throughout the years. We can group them into two categories: 1D and multidimensional. Some comprehensive summaries about 1D models can be found in literature.[4–6] Among the former group we mention the *Granular Diffusion Flame* model by Summerfield,[7] the Hermance model[8] (who proposed a statistic treatment of the oxidizer) and the BDP model by Beckstead et al.[9] (with the attempt to model a combustion process based on multiple flames). All these models solved quickly a set of 1D equations. Heterogeneity treatment, if any, was mainly driven by simple statistical tools. Several developments and refinements are present in literature as well. Nowadays 1D models are still used for rough estimates or as submodels but new efforts are focused onto a multidimensional approach to the problem. 2D and 3D solvers fully dealing with heterogeneity have been worked out in the last few years. We report one paper by Jackson and Buckmaster[10] which is the recapitulation of several former papers about a 3D combustion solver. The model includes 3D fluid dynamics and a simple two-step combustion scheme. Moreover a packing algorithm can be used to model heterogeneity of the solid phase. The solution of the combustion process can be used also as a subgrid model in a full scale rocket simulation.[11] 2D combustion solvers are present in literature as well.[12–14] They have lower requirements in terms of memory and computational resources in spite of more limited capabilities. Nevertheless, if a complex 3D solver is not needed, they allow to focus on some peculiar aspects of the combustion. The present work focuses on nonaluminized propellant flame and modifications occurring when particle size is varied. The intention is to test the capability of a simple 2D combustion model to get those physical changes. At this stage of the work, the verification is mainly qualitative and passes through some comparisons between numerical simulations and real flame images. Combustion movies are taken with a high speed video system. Attention will be given to heterogeneity of the gas phase.

2. Description of the flame and of the numerical model

A comprehensive description of nonaluminized propellant flame is given by Beckstead[9] and an explanatory scheme is reported in Figure 1(a). Beckstead model states the presence of a premixed flame settling just above the AP crystal thanks to its oxidizing decomposition products. A *primary diffusion flame* is present alongside the particle of AP for some of the oxidizing gases diffuse into decomposition products of the binder. This flame does not finish up all reactive components. Finally, leftovers of premixed and primary diffusive reactions mix altogether and generate a *final diffusion flame*. Gas stream is still laminar as reported by Summerfield[7] and as it is visible in Figure 1(b) (snapshot of a propellant combustion with AP size $250\mu m$ and 5 bar) . The combustion model we will apply here is a basic set of 2D equations. It was initially presented by Miccio[12] but some parameters were modified in former works.[2,15] For matter of space we refer to those papers to get the full description of the code.

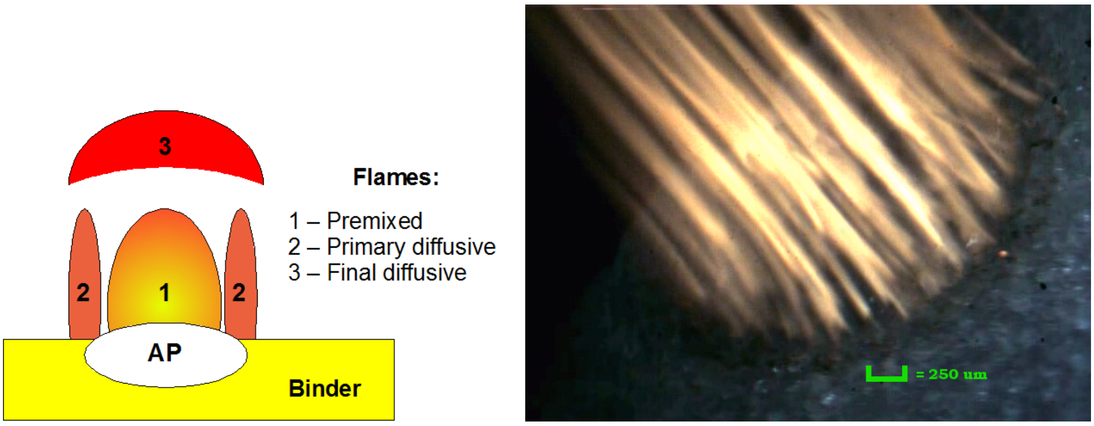

(a) Multiple flames

(b) Propellant combustion at 5 bar

Figure 1: Flame structure

$$\frac{\partial M_g C_g}{\partial t} + \frac{\partial M_g C_g u_x}{\partial x} = 0 \tag{1}$$

where M_g is the molar mass of gas phase which is assumed uniform and constant, C_g is the molar density and u_x is the gas speed along x direction.

$$\frac{\partial Y_i}{\partial t} = -u_x \frac{\partial Y_i}{\partial x} + \frac{\partial}{\partial x} D \frac{\partial Y_i}{\partial x} + \frac{\partial}{\partial y} D \frac{\partial Y_i}{\partial y} + G_i \tag{2}$$

where Y_i is the molar fraction of the i-th component, D is the mass diffusivity and G_i is a source term for the i-th chemical specie.

$$\frac{\partial T}{\partial t} = \left(\frac{\partial}{\partial x} \alpha_g \frac{\partial T}{\partial x} + \frac{\partial}{\partial y} \alpha_g \frac{\partial T}{\partial y} \right) - u_x \frac{\partial T}{\partial x} - \frac{1}{C_g \gamma_g} (r_4 \Delta h_4 + r_5 \Delta h_5) \tag{3}$$

where T is the temperature in Kelvin, γ_g is the specific heat, α_g is the thermal diffusivity and Δh_i is the enthalpy of i-th reaction that evolves with rate r_i.

$$C_g = \frac{p}{\Re T} \tag{4}$$

where p is the pressure[16] and $\Re$ is the universal constant of gas expressed in $J/(\mathrm{mol}\, K)$. The fluid is inviscid. The stream is laminar and 1D motion equations are adopted (Equation 1). Chemical species conservation is performed by a 1D transport and 2D diffusion model (Equation 2). Hypothesis of perfect gas is assumed (Equation 4). Heat transfer is computed inside the solid phase (Eq. 5).

$$\frac{\partial T}{\partial t} = \frac{\partial}{\partial x} \alpha_s \frac{\partial T}{\partial x} + \frac{\partial}{\partial y} \alpha_s \frac{\partial T}{\partial y} \tag{5}$$

Virgin propellant maintains both chemical and physical heterogeneity so that burning surface composition can change in space and time reflecting the displacement of reactants in the bulk. Reactivity is confined on the gas-solid interface and inside the gas domain while we assume that the bulk is still nonreactive. Five global reactions set up the combustion model which controls the reactivity inside the gas phase and the regression rate of the condensed matter as well.

$$\text{R1: } A_s \rightarrow 10B_g \qquad r_{r-1} = A_1 \exp\left(\frac{-E_{a-1}}{\Re T_s}\right) \tag{6}$$

$$\text{R2: } C_s \rightarrow D_g + E_g \qquad r_{r-2} = A_2 \exp\left(\frac{-E_{a-2}}{\Re T_s}\right) \tag{7}$$

$$\text{R3: } 1/5A_s + E_g \rightarrow 4F_g \qquad r_{r-3} = A_3\, Y_E \frac{p}{\Re T} \exp\left(\frac{-E_{a-3}}{\Re T_s}\right) \tag{8}$$

$$\text{R4: } D_g + 1/2E_g \rightarrow 2F_g \qquad r_{r-4} = A_4\, p^{1.8}\, Y_D\, Y_E \exp\left(\frac{-E_{a-4}}{\Re T}\right) \tag{9}$$

$$\text{R5: } B_g + 1/2E_g \rightarrow 2F_g \qquad r_{r-5} = A_5\, p^{1.5}\, Y_B\, Y_E \exp\left(\frac{-E_{a-5}}{\Re T}\right) \tag{10}$$

where E_{a-i} is the activation energy and A_i is the pre-exponential term. The specie A depicts the binder. C is the oxidized. B, C, D and E are intermediate products and F is the final species. This reaction scheme is by far simpler than fully resolved kinetics despite captures some essential aspects of the combustion process. Equations 6 and 7 represent the decomposition of binder and oxidizer. Equation 8 is a heterogeneous reaction between solid binder and oxidizing gas species. Equation 9 is the premixed combustion while Equation 10 traces all the diffusive reactions. 2D domain is plot in figure 2 together with axes orientation. Laminate propellant configuration is chosen to get rid of unsteadiness inside the flame structure. The use of a random AP displacement in the bulk should get a more representative propellant but surface composition should change during combustion. Laminas of different thickness are used though the AP/HTPB mass ratio is always 80/20. Boundary conditions consist of null derivatives on sides as well as on top of the domain for all variables. Ambient temperature is set at the bottom of the solid phase. The gas-solid interface moves over because of the material consumption. There, a couple of boundary conditions are still missing for the gas phase. Regression rate is treated according to the local composition by Equations 6 and 7. Those reactions also assign the boundary condition for chemical composition of gas phase. One more condition is set over there for gas speed by the relation 11.

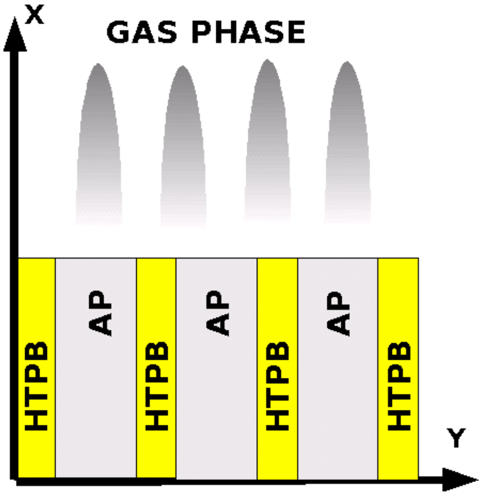

Figure 2: Computational domain: laminate propellant

$$u_{x-loc} = \frac{\rho_{s-loc} r_{b-loc}}{\rho_{g-loc}} \tag{11}$$

with ρ as local density and r_b the local consumption rate of the solid phase. Thermal balance across gas-solid interface includes also surface reactions and is given by the equation 12.

$$k_g \frac{\partial T}{\partial n} = k_s \frac{\partial T}{\partial n} - (r_{r-1}\Delta h_1 + r_{r-2}\Delta h_2 + r_{r-3}\Delta h_3) \tag{12}$$

defining k as thermal conductivity.

3. Real propellant combustion

Some nonaluminized propellants with different powder size ϕ were worked over with a high speed video recording technique. AP/HTPB mass ratio for any of those propellants was 80/20. No addition of compatibilizing agents as well as burning catalysts was done. Each propellant contains one of the following powder cuts:

- Fine cut: $\phi_f = 5 - 10\,\mu m$
- Intermediate cut: $\phi_m = 80 - 140\,\mu m$
- Coarse cut: $\phi_c \approx 400\,\mu m$.

Selection of ϕ_m was done with sieves while ϕ_c and ϕ_f come from an industrial supplier. Combustion tests were run inside a horizontal bomb filled up with nitrogen at a defined pressure in the range $1 - 15\,bar$. The steel container has a volume of a couple of liters and has some optical accesses. The facility comprises a laser system and a controlled exhaust system. The laser beam grants the ignition acting as non intrusive heating source while a set of automatic valves retains the pressure inside a narrow range even during combustion. Camera is placed aside, along with a long range microscope and a cold light source. The absence of metal leads to darker flame with respect to metalized formulations. Thus, frame rate must be limited to 500 fps for matter of visibility.

4. Frames from experimental tests

In the following pictures we report some frames taken from propellant combustion movies. Figure 3 refers to the pressure of 1 bar while Figure 4 is for 15 bar combustion. As we substitute a coarser AP cut (Figures 3(b) and 4(c)) with a finer one (Figures 3(a) and 4(a)), the flame becomes more regular and uniform. The combustion at 1 bar of propellants containing coarse AP features long and separate flames unlike material with fine AP which shows a well-mixed reaction field. The magnification of one single flame for coarse AP combustion is shown in Figure 3(c). Flame dimension is close to crystal size so we may argue that it may spring from one single particle. Similar discussion can be done for combustion at higher pressure though the overall flame length is reduced for all cases. Besides, the process is faster and it becomes difficult to get clear and detailed images.

5. Application of combustion model

Here we apply on some laminate propellant configurations (Figure 5) the model detailed in Section 2. Model combustion is performed at 60 bar with three different AP lamina sizes: $56\,\mu m$, $140\,\mu m$ and $500\,\mu m$. Kinetic scheme features low pressure sensitivity. Unfair burning rate prediction still requires some tuning of chemistry, mainly to set up a proper pressure dependence.

Conversely, the physical model catches the governing features of the flame and the correspondence between temperature fields and flame visualization is good. Model simulation for coarser AP represents a heterogeneous flame. The use of $500\,\mu m$ AP (Figure 5(b)) produces a structure that is similar to the detailed view reported in Figure 3(c). In this case, side diffusion of reactants is a slow process and does not allow a proper mixing close to the burning surface. Flame structure is stretched along the stream direction. Only the primary diffusion flame is present in this case. Despite the numerical solution does not get the final diffusion flame for this case, experimental pictures suggest that the final flame occurrence is located far from the burning surface, therefore out of domain. Mixing capability increases with the use of finer laminas (Figure 5(b)). In this case, side diffusion brings reactant blending nearer to the gas-solid interface. Heterogeneity of the solid phase reduces its influence on gas side because final diffusion flame is getting closer to burning surface as the AP laminas are decreased in size. The field appears to be uniform over the final diffusion flame. Primary diffusion and premixed flames are too short to be observed clearly. Moreover, the use of very fine AP tends to produce a flat final flame. In this case reactant diffusion might be fast enough to homogenize gas phase before any reaction and premixed flame could occur. An experimental representation of this case is given in Figure 3(a). Combustion movies taken at a higher pressure depict the same trend albeit it is not as evident as for experiments at 1 bar.

6. Conclusion

Experimental and modeling activities were performed on nonaluminized propellants. The focus of the work was posed on the flame shape and its inner structure. Some propellants were manufactured and combustion movies were taken. Laminate propellant configuration was also tested with a simplified combustion model. Influence of oxidizing

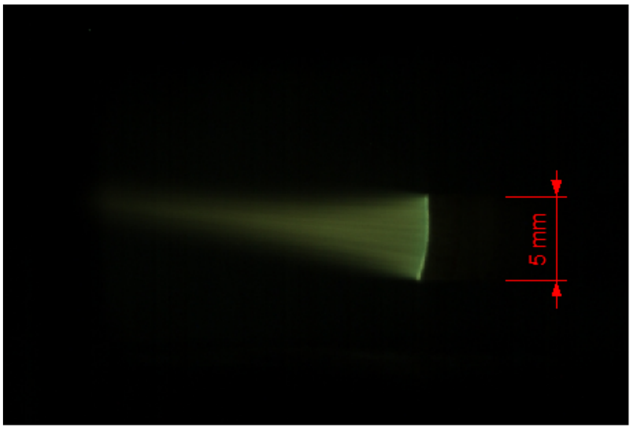

(a) Propellant with ϕ_f cut

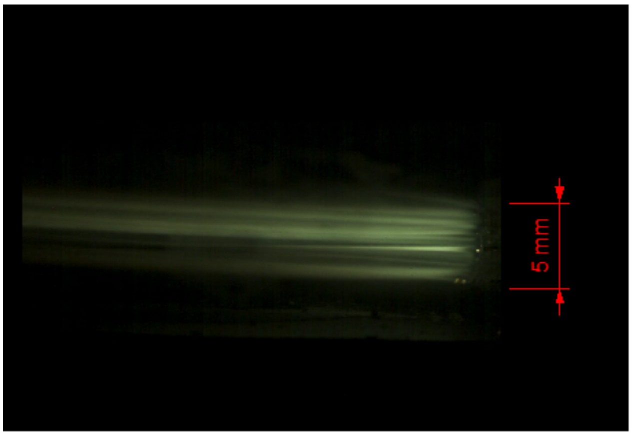

(b) Propellant with ϕ_c cut

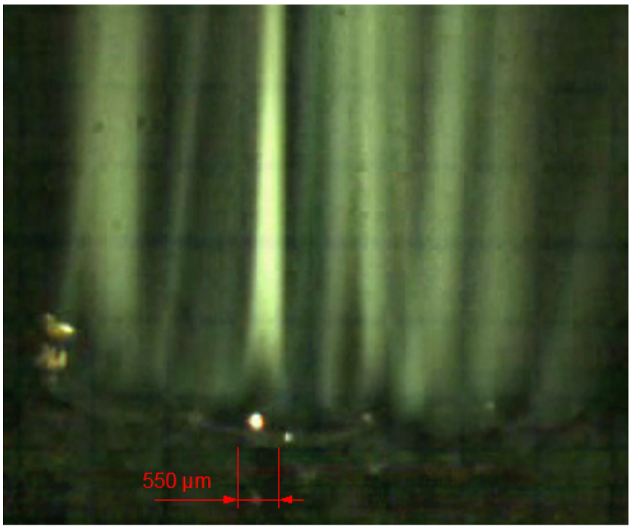

(c) Detail of propellant combustion with ϕ_c cut (graph paper size 1 mm)

Figure 3: Combustion performed at 1 bar

(a) Propellant with ϕ_f cut

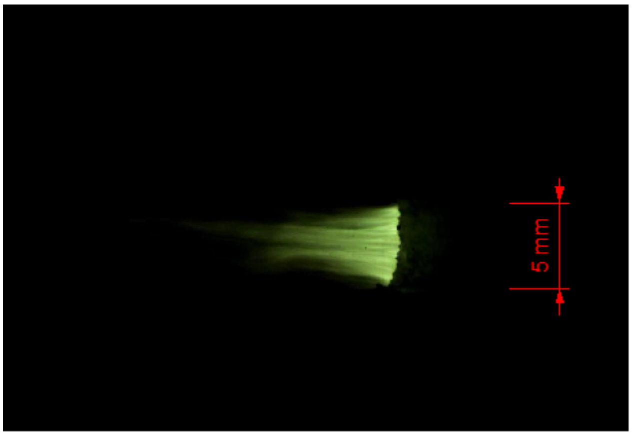

(b) Propellant with ϕ_m cut

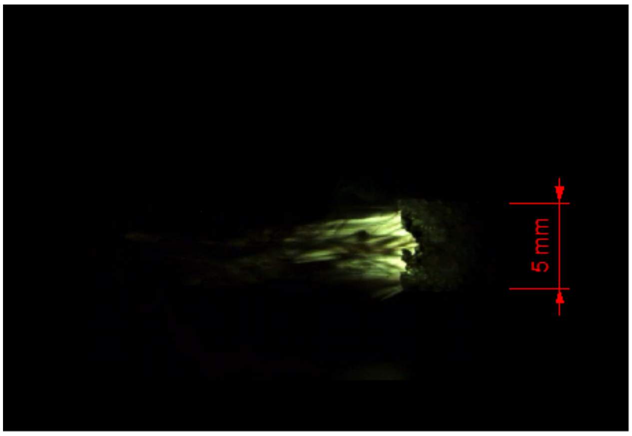

(c) Propellant with ϕ_c cut

Figure 4: Combustion performed at 15 bar

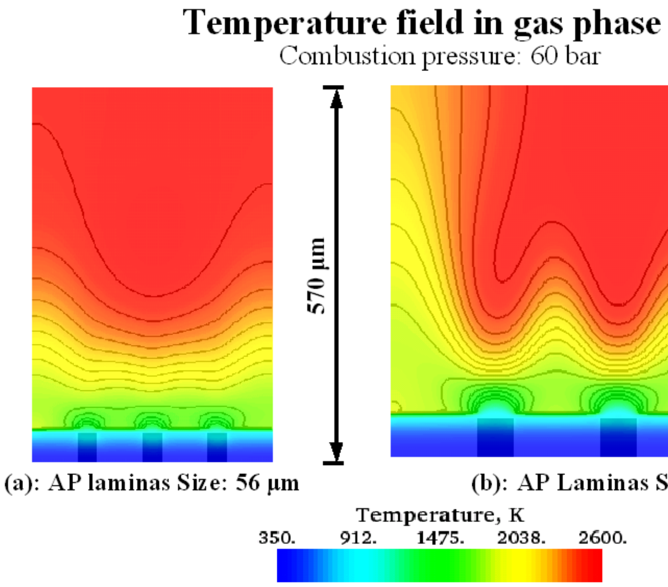

(a) Laminas of size 56 μm and 140 μm

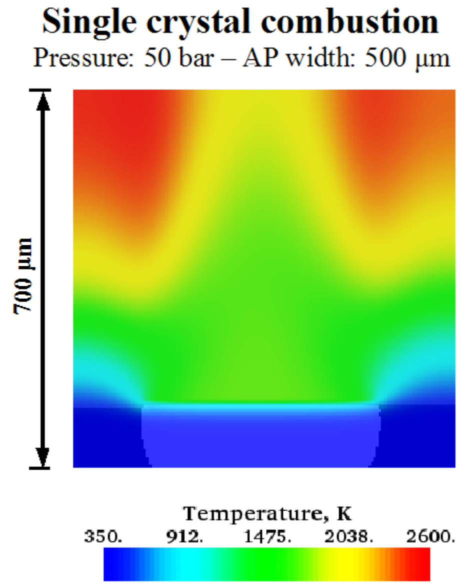

(b) Crystal of size 500 μm

Figure 5: Laminate propellant combustion: temperature field

particle size was traced with qualitative observations and both experiments and modeling agreed on the flame structure modifications. As particle size was reduced, a progressive enhancement in mixing process was observed. The trend leaded to homogenize the gas phase before any reaction. In this case, upcoming flame should be premixed but we need further experiments and simulations to get a comprehensive analysis on that. This work suggested that a simplified model like Miccio's should be able to catch the essentials of the combustion process though some refinement should be needed, especially in the chemical scheme. In fact, it is still necessary to ensure better prediction capabilities of combustion macroscopic features like burning rate.

References

[1] T. L. Boggs. Deflagration rate, surface structure and subsurface profile of self-deflagratingsingle crystals of ammonium perchlorate. *AIAA Journal*, 8(5):867–873, 1970.

[2] F. Maggi, L. Galfetti, F. Miccio, and L. T. De Luca. Flame structure simulation of nonaluminized composite propellants. In *57th International Astronautical Conference*, No. IAC-06-C4.P.3.03, pages 1–14, Valencia, Spain, October 2006. IAF.

[3] H. Arisawa and T. B. Brill. Flash pyrolysis of hydroxyl-terminated polybutadiene (HTPB) I: Analysisand implications of the gaseous products. *Combustion and Flame*, 106:131–143, 1996.

[4] K. N. R. Ramohalli. Steady state burning of composite propellants under zero-cross flow situation. In K. K. Kuo and M. Summerfield, editors, *Fundamental of Solid Propellant Combustion*, No. 90 in Progress in Astronautics and Aeronautics Series, pages 409–477, New York, NY, USA, 1984. AIAA.

[5] N. S. Cohen. Review of composite propellant burn rate modeling. *AIAA Journal*, 18(3):277–293, 1979.

[6] K. Kishore. Comprehensive view of the combustion models of composite solid propellants. *AIAA Journal*, 17(11):1216–1224, 1979.

[7] J. A. Steinz, P. L. Stang, and M. Summerfield. The burning mechanism of ammonium perchlorate-based composite solid propellants. Technical Report 830, Princeton University, Department of Aerospace and Mechanical Sciences, 1969.

[8] C. E. Hermance. A model of composite propellant combustion including surface heterogeneityand heat generation. *AIAA Journal*, 9(4):1629–1637, 1966.

[9] M. W. Beckstead, R. L. Derr, and C. F. Price. A model of composite solid-propellant combustion based on multiple flames. *AIAA Journal*, 8(12):2200–2207, 1970.

[10] T. L. Jackson and J. Buckmaster. Heterogeneous propellant combustion. *AIAA Journal*, 40(6):1122–1130, 2002.

[11] L. Massa, L. T. Jackson, and J. Buckmaster. Using heterogeneous propellant burning simulations as subgrid componentsof rocket simulations. *AIAAj*, 42(9):1889–1900, 2004.

[12] F. Miccio. Numerical modeling of composite propellant combustion. In *27th International Symposium on Combustion*, pages 2387–2395, The Combustion Institute, 1998.

[13] S. Groult and A. Bizot. Numerical simulation of heterogeneous AP-HTPB propellant combustion. In *40th AIAA/ASME/SAE/ASEE Joint Propulsion Conference and Exhibit*, No. 2004-4039, Fort Lauderdale, FL, USA, 2004.

[14] R. Cazan and S. Menon. Direct numerical simulation of sandwich and random-packed propellant. In *39th AIAA/ASME/SAE/ASEE Joint Propulsion Conference*, No. 2003-5082, Huntsville, AL, USA, 2003.

[15] F. Maggi, F. Miccio, and L. T. DeLuca. Effects of heterogeneity on flame structure of AP-HTPB propellants. In *European Conference of Aero-Space Sciences*, Moscow, Russia, 2005.

[16] P. Clavin. Premixed combustion and gasdynamics. *Annual Review of Fluid Mechanics*, 26:321–352, 1994.